# Geophysical Techniques for Monitoring Settlement Phenomena Occurring in Reinforced Concrete Buildings

**L. Capozzoli**[1] (ORCID) · **G. De Martino**[1] · **M. Polemio**[2] · **E. Rizzo**[1]

## Abstract

Geophysical investigations could provide a valid tool for the identification of possible causes of settlement phenomena that affect civil buildings. They provide a non-invasive method of obtaining high-resolution information about the subsoil, saving time and money. However, uncertainties related to the accurate interpretation of the acquired data could potentially reduce the value of these methods. For this reason, the integration of non-invasive tests with direct measurements to support geophysical data interpretation is strongly recommended. This is a fundamental step in the process of defining a sufficiently reliable geological model to explain the cause of failure. Among the various geophysical techniques, electrical resistivity tomography and ground penetrating radar offer significant advantages for monitoring the status of the conservation of civil engineering structures and infrastructures. This paper presents the most recent and beneficial advances of the use of electric and electromagnetic geophysical methods in the field of civil engineering, with particular attention to their applications for monitoring subsidence and settlement phenomena. Finally, the possibilities of the joint use of resistivity and electromagnetic methods for studying the causes of the structural decay that affects two precast buildings are monitored and discussed. The results demonstrate the capability of combining non-destructive geophysical techniques with direct data, for evaluating the safety of building constructions and solving geotechnical problems.

**Keywords** Engineering geophysics · Non destructive testing (NDT) · Electrical resistivity tomography (ERT) · Ground penetrating radar (GPR) · Settlement phenomena · Reinforced concrete (RC) structures · Geotechnical application

✉ L. Capozzoli
   luigi.capozzoli@imaa.cnr.it

1   CNR-IMAA, National Research Council, Institute of Methodologies for Environmental Analysis, 84050 Tito, PZ, Italy

2   CNR-IRPI, National Research Council – Research Institute for Hydrogeological Protection, Bari, Italy

# 1 Introduction

The requirement to investigate civil structures and infrastructures in non-invasive ways represents an important challenge for the scientific research if it is to minimize the impact of the analysis and maximize the quality of obtainable results, in terms of resolution and depth of investigation. The checking and maintenance operations for assessing a building's conditions require high resolutions and continuous procedures that are repeated over long time periods, without interrupting the normal life of the monitored construction. For these reasons, non-destructive tests are widely applied in the engineering field. Among the various techniques, sonic tests and thermal infrared readings provide useful information about the state of the conservation of structures or elements (Maldague 2001).

Geophysical investigations are widely used for the analysis of subsoil before engineering construction design activities commence. In recent years, the large number of applications of geophysical techniques in the field of engineering has led some authors to define this new branch of research "Urban Geophysics" (UG). UG is based on the use of non-invasive or low-invasive techniques, or a combination of both, for testing engineering structures or identifying the causes of the deterioration in structures (Verma and Sharma 2011). UG analyses issues are caused by the presence of natural and anthropic noise that obviously exists in industrialized and urban areas and might considerably reduce the value of measurements (Williams et al. 2006; Lapenna 2016).

In this perspective, among the different techniques used to survey the subsoil before construction activities commence, the most frequently adopted are the seismic methods and microtremor measurements. The popularity of these methods is related to their ease of use in the evaluation of the seismic response of the subsoil and the effectiveness of predicting the physical characteristics of the soil (Martínez and Mendoza 2011; Krawczyk et al. 2013; Mokhberi 2015).

Unfortunately, because of their limits in terms of resolution and depth of investigation, electric and electromagnetic techniques are less commonly used for geotechnical purposes. This is also the case for electrical resistivity tomographies (ERT) and ground penetrating radar (GPR) which could be playing a very important role in UG. Indeed, despite the wide use of these methods in other fields of engineering, their use in geotechnical applications is not systematic and often neglected. Because of the non-invasive methods that GPR and ERT use to provide information regarding the safety of constructions, they are well suited for surveying foundation soils and identifying possible causes of settlement. Furthermore, since they are both cheaper and faster than direct measurement, they could be effectively applied to support geological models that are based solely on geotechnical drilling and seismic information (refraction tests, multichannel analysis of surface waves (MASW), and refraction microtremor (REMI), etc.).

However, there are some limits that restrict the use of these techniques, such as:

a. individual requirements of the situation that necessitate the use of direct data to constrain the interpretation;
b. a limited depth of investigation or a resolution that does not meet requirements;
c. where installation or use in specific industrial and urban environments is difficult and time consuming

The most frequently encountered advantages and disadvantages of ERT and GPR are indicated in Table 1. In any case, their integrated use is suggested in order to reduce the limits and enhance the advantages of each technique.

**Table 1** Limits and potentialities of Ground penetrating radar (GPR) and Electrical resistivity tomography (ERT) in engineering applications

| | GPR | | ERT | |
|---|---|---|---|---|
| | Limits | Advantages | Limits | Advantages |
| Resolution | Frequency dependent | Adequate for engineering applications | Array dependent | From metres to some tens of metres |
| Depth | Frequency dependent | From few centimetres to some metres | Electrode distance and array dependent | From metres to some tens of metres |
| Time (required from the test) | Depending on the size target 3D acquisitions very time-consuming | Really fast if compared to the direct measurements | Depending on the size target 3D acquisitions extremely time-consuming | Really fast if compared to the direct measurements |
| Integration with NDT (Infrared thermography IRT, Acoustic tests AT, magnetic tests, etc.) | Low with seismic acquisition and ERT | Good integration with IRT, AT and other magnetic tests | Low- with high-resolution techniques (IRT, AT and GPR) | High with seismic prospection |
| Repeatability | Hard in the absence of automated systems of acquisition | High resolution for monitoring physical variations | Check of electrode positioning and contact resistance | Easy for 4D borehole and surface acquisition |
| Applicability | Rough or not homogeneous surface | Fast in absence of obstacle and smooth surfaces | Dry soils or non-conductive medium could obstacle the acquisitions | Relatively easy data acquisition and processing |
| Information | Quantitative information requires more complex data processing | High detail for identifying positions of reflectors for engineering issues | Resistivity data require necessarily the inversion of the acquired data | High sensitivity to water content variations or presence of voids |

The aim of this paper is to provide an overview of ERT and GPR applied for analysing structural engineering elements (laboratory tests on samples and specimens) when investigating the decay of both old civil engineering structures (foundations, piles, beams, columns, etc.) and infrastructures (dams, roads, bridge decks, etc.). The paper describes the theoretical elements of the two techniques and, more importantly, the advantages of an integrated approach. Additionally, results obtained through the combined use of GPR and ERT for monitoring two test sites are discussed in order to demonstrate the potential of these methods for monitoring settlement occurring in precast reinforced concrete (RC) buildings in urban and industrialized contexts.

## 1.1 Electrical Resistivity Tomography

ERT is an active geophysical method which involves the introduction of direct current (DC) by a pair of electrodes placed on the ground (current electrodes) and the recording of the subsequent drop in potential using a second pair of electrodes (potential electrodes). This well-known technique is based on the use of Ohm's law, and its purpose is to monitor and classify the electrical behaviour of the subsoil caused mainly by its porosity and water content.

Generally, the applied and recorded signals are switched square waves (Binley and Kemna 2005) and an advanced "multimeter", the georesistivimeter, is used to detect the precise drop between the potential and current electrodes. In homogeneous ground, the current flows radially out from the current source and the resulting equipotential surfaces run perpendicular to the current flow lines, generating hemispheres. In other cases, the current flow lines and the equipotential lines are distributed in complex forms depending on resistance caused by the nature of the ground (see Fig. 1). From the data acquired, the apparent resistivity ($\rho_a$) is calculated as follows:

$$\rho_a = \frac{\Delta V}{I} k$$

where $\Delta V$ is the measured potential (mV), $I$ the transmitted current (mA) and $k$ the geometric factor depending on the type of electrode array used (m). Different position configurations of each pair of electrodes (both current and potential) can be used. The most common are Wenner–Schlumberger and dipole–dipole arrays.

The Wenner array is composed of four equidistantly placed electrodes. With "$a$" the distance between each pair of adjacent electrodes, the geometry factor ($k$) is calculated as follows:

$$k = 2\pi a.$$

The Wenner–Schlumberger is a hybrid array that combines features of both the Wenner and Schlumberger arrays; in this case, $k$ is expressed as:

$$k = \frac{\pi}{a} \left[ \left( \frac{L}{2} \right)^2 - \left( \frac{a}{2} \right)^2 \right]$$

where $L$ is the distance between the current electrodes (AB) and $a$ the distance between those of the potential (MN).

The dipole–dipole array works with two pairs of electrodes, one for the current and the other for the potential. The geometric factor depends on the distance between each
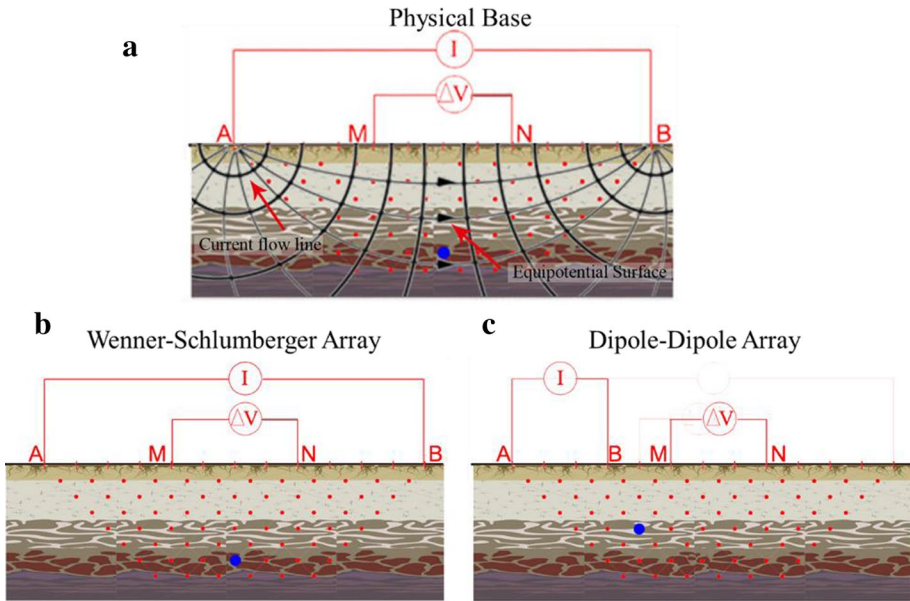
**Fig. 1** Operating principle of ERT (**a**) with the Wenner–Schlumberger (**b**) and dipole–dipole (**c**) electrode arrays used for common geoelectrical investigations. A and B represent the current electrodes and M and N the potential electrodes

electrode. The "classic" linear dipole–dipole configuration has a geometrical factor equal to:

$$k = \pi n a(n + 1)(n + 2)$$

where $a$ is the distance between each current and potential electrode, $n$ the dipole separation factor and $na$ the distance between the pairs of current electrodes and potential electrodes.

The apparent resistivity values are transformed into actual resistivity and depth by means of an inversion algorithm. The aim of the inversion procedure is to compute the "best" set of resistivity values, to satisfy both the measured data set and some a priori constraints, in order to stabilize the inversion and constrain the final image (de Groot-Hedlin and Constable 1990).

As described by Loke (2000), the array is chosen according to: (1) the type of target (sizes, depth, physical characteristics); (2) the sensitivity of the array to vertical and horizontal changes in the subsurface resistivity; (3) the background noise level; (4) the depth of investigation required; and (5) the necessary signal strength. Dipole–dipole, Wenner and Schlumberger arrays are able to reach a depth range of between 0.15 and 0.2 times the total length of the investigated line (L). A fundamental factor in order to understand the capability of each array is the sensitivity that describes the spatial distribution of electric potential in the subsurface. This parameter varies strongly according to the used array. The Wenner array obtains a good resolution for vertical variations but it is limited for monitoring horizontal changes. On the other hand, the dipole–dipole array is very sensitive to horizontal changes in resistivity, but relatively insensitive when resolving vertical changes. The Wenner–Schlumberger array could represent a good compromise for most general applications

in engineering and geotechnical fields, as it is moderately sensitive to both horizontal and vertical structures (Furman et al. 2003).

The application of ERT in urban or industrialized areas is often limited by structures that prevent easy acquisition of data (houses, paved roads, monuments, etc.), the presence of asphalt in particular, due to its electrical insulating properties. In this case, the creation of small holes filled with bentonite and salt solution is required to produce acquisitions. In addition, the presence of buildings can limit the use of linear ERT profiles; in fact, in urban and industrialized environments, it should be accepted that the area available for measurements is restricted and that the reduction in length will result in a decrease in the investigation depth. The use of electrodes placed along lines perpendicular to each other can, however, efficiently reduce this problem (Szalai et al. 2011).

Finally, it is worth noting that the application of resistivity methods in engineering fields is less common than other geophysical techniques, in particular for assessing the safety of buildings as they are constructed. The main reasons for this are related to the high resistance of contact between the electrodes and the medium being investigated: the obtainable resolution is often not sufficient for engineering applications. Despite these limitations, the authors of this paper would like to suggest the importance of ERT methods in urban areas when integrated with more common urban procedures for monitoring engineering structures and infrastructures.

### 1.1.1 Concrete Sample Testing

The starting point for understanding the usefulness of ERT in engineering fields is the strong physical relationship that exists between the porosity of construction materials (concrete, stone, wood, etc.) and their electrical behaviour.

One of the earliest engineering issues where ERT was applied is discussed by Hunkeler (1996). The author studied and compared the resistivity of mortar, concrete and their pore solutions, demonstrating their importance in the understanding of rebar corrosion phenomena. Subsequently, other researchers analysed the potential of ERT for monitoring the decay of RC elements and structures. Lataste et al. (2003) adopted the resistivity method, supported by numerical simulation, to monitor crack phenomena occurring in reinforced concrete structures. Their results were validated with experimental tests conducted on concrete slabs of limited sizes affected by cracks and areas of delamination. Using a similar approach, Wiwattanachang and Giao (2011) monitored cracks in fibre-reinforced concrete beams using ERT. Since electrical techniques are able to monitor the presence of water, the authors demonstrated that it is possible to study the curing process of the concrete. Laboratory tests on concrete specimens have allowed the monitoring of concrete resistivity development over time. The compressive strength was observed simultaneously to resistivity variation. Du Plooy et al. (2013) have also designed and built prototype instrumentation based on electrical resistivity measurements to assess the conditions of concrete samples in laboratory tests. The aim of this research was to identify potential master curves between DC resistivity value and the parameters indicative of concrete condition (water content, chloride content and porosity). Bonnet and Balayssac (2018) have analysed the carbonation depth and saturation level of concrete, demonstrating the usefulness of the electrical method in combination with a surface permeameter. The results of the analysis undertaken on small samples in laboratory conditions show the capability of ERT methods in predicting the water content of each concrete sample.

### 1.1.2 Civil Engineering Structures and Infrastructures

In addition to laboratory tests, application of ERT in restoration and engineering fields demonstrates its usefulness when testing the condition of masonry walls and RC structures. Buettner et al. (1996) have used several ERT boreholes to image spatial moisture distribution and movement in pavement sections during an infiltration test. The case analysed showed the importance of this innovative approach that provides a consistently high resolution for imaging subsurface engineering structures, overcoming the effects of a loss in resolution of conventional surface acquisitions.

Flint et al. (1999) have used ERT in tandem with seismic measurements to monitor the internal state of a masonry viaduct. The authors highlighted how the resistivity method is highly sensitive to changes in internal moisture content, which makes it an ideal technique for the long-term monitoring of water ingress in masonry structures.

Keersmaekers et al. (2004) successfully demonstrated the use of geo-electrical survey in the field of restoration. The authors monitored the internal structure of masonry walls and validated the results with endoscopic measurements. ERT has also been successfully implemented to control work when consolidating column foundations (Keersmaekers et al. 2008). As regards the use of ERT aimed at monitoring the conditions of masonry walls, Van Rickstal et al. (2008) analysed the electrical behaviour of a limestone medieval tower, supported by endoscopic measurements, to identify decay of the structure. For this purpose, the cross-borehole configuration was tested for monitoring grout injection work on a masonry structure in laboratory conditions. In the same context, Sass and Viles (2006, 2010) used ERT to investigate the progress of moisture absorption and evaporation in ancient masonry walls. They have also demonstrated that the resistivity method is able to identify the cause of decay affecting stone blocks; with the support of ERT, they concluded that materials with highly weathered surfaces have the most rapid and highest levels of water uptake. Therefore, the use of ERT is particularly suitable for analysing the moisture content of deteriorating masonry walls.

Engineering fields also integrate ERT with other geophysical methods. Capozzoli and Rizzo (2017) have tested the use of ERT in tandem with subsurface measurements to identify the presence of voids and cracks in concrete slabs reinforced with electrically welded mesh. Loperte et al. (2016) have integrated ERT with thermal infrared mapping and ground penetrating radar in order to monitor seepage phenomena occurring in a rock-fill dam. ERT is also successfully used for monitoring the subsoil on a larger scale in order to detect buried cavities (Cardarelli et al. 2006; Guérin et al. 2009; Ungureanu et al. 2017), analyse hydrogeological systems (Martel et al. 2018), or monitor geological hazards such as landslides and sinkhole collapses (Gómez-Ortiz and Martín-Crespo 2012; Giampaolo et al. 2016; Sevil et al. 2017).

## 1.2 Ground Penetrating Radar

GPR is one of the most popular near-surface geophysical methods. It is based on the introduction of electromagnetic (EM) waves that are able, in the presence of variations in EM impedance of the investigated medium, to identify anomalous phenomena occurring in the subsoil (see Fig. 2). In detail, variations in the physical properties of the investigated medium such as dielectric permittivity ($\varepsilon$, $F$/m), electrical conductivity ($\sigma$, $S$/m) and magnetic permeability ($\mu$, $H$/m) are recorded as reflections characterized by a particular
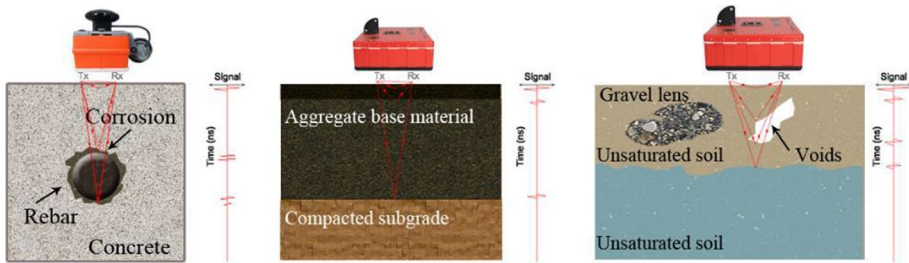
**Fig. 2** Operating principle of GPR acquisitions for monitoring engineering issues like corrosion rebar, asphalt road and geological contexts

amplitude or phase. Variations in physical properties significantly influence the velocity of propagation of EM waves and energy attenuation. Analyses of variations in velocity are used to create permittivity maps according to the fundamental relationship for non-dispersive medium

$$v = \frac{c}{\sqrt{\varepsilon}}$$

where $v$ is the propagating velocity of the material, $c$ is the velocity of EM waves in the void ($2.998 \times 10^{-1}$ m s$^{-1}$) and $\varepsilon$ represents the relative permittivity of the material (Annan 2005). It is possible to evaluate the velocity, and therefore the dielectric permittivity, with direct or indirect methods. The application of the former is very difficult to use in actual situations because it is often not possible to create trenches or excavate in order to place reflectors in the soil; it is far easier to apply an indirect system of measurement, based, for example, on the study of the hyperbolas generated by reflectors located in the investigated medium. Imaging of the subsoil in terms of dielectric permittivity is an effective aid in identifying more humid (high values of $\varepsilon$) and drier (low values of $\varepsilon$) areas (Moore et al. 1999; Cassidy 2009).

The instrumentation used for GPR is generally composed of an acquisition unit (a laptop or similar) and one or more antennas that work as both transmitter and receiver (bistatic model) or only as either a transmitter or a receiver (monostatic). The antenna plays a key role in GPR analysis since it regulates the resolution and depth of acquisition, and its choice needs great care, taking into account the target's characteristics in terms of size, depth and physical properties (Daniels 2004).

The growing interest in GPR in the field of engineering is related to the high resolution offered by the method when used for laboratory tests, carried out on samples and specimens, as well as for field investigations.

GPR is particularly useful in various engineering and geotechnical/geological applications, particularly when detecting the presence of defects, cracks or delamination induced by the corrosion of rebar. GPR generates reflections that provide useful information about the state of conservation of reinforced concrete elements. Indeed, because the dielectric permittivity of air ($\varepsilon = 1$) is considerably lower than concrete ($\varepsilon = 4$–15), the reflections at the air–concrete interface close to the deteriorated rebar are obvious and easily detectable. GPR is also a powerful tool to categorize and monitor multilayer engineering structures (e.g., roads or buildings) and geological contexts. In these cases, variations in dielectric permittivity and electrical conductivity provide a way of identifying defects or

inhomogeneity affecting the subsoil. In correspondence with each variation of the physical parameters, a reflection of the GPR signal is recorded and the attenuation of the EM signal can be used to study the physical characteristics of the investigated medium (Jol 2008).

### 1.2.1 Laboratory Tests

Numerous papers have recorded laboratory tests that demonstrate the usefulness of GPR for analysing corrosion occurring in engineering structures. Dérobert et al. (2008, 2017; Dérobert and Villain 2017) monitored chloride contamination (attributed to the corrosion of rebar) in concrete using a combination of electromagnetic, resistivity and capacitive techniques. The presence of moisture, or water, strongly influences the electromagnetic behaviour of the concrete, generating variations for the two physical parameters of interest in GPR: electrical conductivity and dielectric permittivity.

Viriyametanont et al. (2008) analysed the possibility of estimating concrete porosity and water content by assessing the direct wave-time position; tests performed on small samples in the laboratory showed that wave-time position is directly affected by variations in concrete porosity and water content.

Laurens et al. (2007) highlighted the relationship between the characteristics of the direct waves generated by a GPR antenna and the degree of pore saturation and/or the resistivity of concrete. The experiments were carried out on a variety of $25 \times 25 \times 7$ cm concrete specimens. Great efforts were made by the authors to identify an experimental relationship between the electrical resistivity of concrete and the amplitude of the direct wave.

### 1.2.2 Civil Structures and Infrastructures

The ability to apply GPR when analysing the state of conservation of structural elements belonging to civil engineering structures and infrastructures is also important. Some authors (Dérobert et al. 2002; Hugenschmidt and Mastrangelo 2006; Hugenschmidt et al. 2013; Alani et al. 2014) have successfully used GPR to monitor the conditions of RC structures, such as post-tensioned beams, rail track and bridges. In this context, an interesting contribution was offered by Proto et al. (2010) that proposed the integrated use of different non-destructive tests, including GPR, for providing information about the state of conservation of engineering structures (beams, bridges, etc.).

GPR is widely used to assess road condition (Benedetto and Pensa 2007; Tosti and Umiliaco 2014; Benedetto et al. 2009; Tosti and Slob 2015). The ability to accurately assess the geometrical and mechanical properties of civil engineering infrastructures using GPR is demonstrated by Tosti et al. (2018), who proposed an experiment-based model for qualitatively studying the stiffness of flexible pavement using a tandem arrangement of GPR horn antenna and light falling weight deflectometer. In this context, Loizos and Plati (2007) have demonstrated the capability of GPR for estimating, with some accuracy, pavement thickness. The paper compared the GPR results on asphalt cores collected in field studies with those obtained in a laboratory using a percometer, an instrument capable of estimating the dielectric constant and specific conductivity of materials. Shangguan et al. (2016) faced another important challenge regarding the monitoring of roads with GPR. They demonstrated that GPR is also able to assess the density of asphalt pavement with the adoption of a correction algorithm, based on a reference scan approach that has proved to significantly reduce prediction errors.

### 1.2.3 Underground Utilities

A key area of research in the application of GPR is where it is widely used for the localization of underground utilities placed at different depths in the subsoil (Plati and Dérobert 2015). Lai et al. (2018) describe various applications of GPR, highlighting the importance for mapping underground utilities in urban contexts both for plastic water pipe leak detection and for detecting voids under roadways and concrete sections of underground utilities. Sagnard et al. (2016) highlighted the problems relating to uncertainties when using GPR acquisitions for utility detection. They designed and built a test site with objects of known size placed at different depths for studying the capability of GPR to investigate, in time and frequency domains, physical phenomena induced by dielectric and conductive utilities, while also monitoring the polarization of the signal for the detection and identification of buried objects. Numerical modelling and 3D reconstructions were realized with several types of algorithm, along with quantitative information about the depth of the buried objects. Liu et al. (2018) proposed an interesting approach where a wide-band GPR system is used for the detection and location of the junctions that connect buried power cables. The results, supported by numerical simulations and actual measurements, also showed the capability of GPR for monitoring specific utilities.

### 1.2.4 Cultural Heritage

GPR is widely used for investigating archaeological sites, often in tandem with other geophysical techniques (Capozzoli et al. 2015; Masini et al. 2018; Rizzo et al. 2018). At the same time, it offers great advantages for the evaluation of the condition of historic structures by exploiting its non-invasive nature (Masini et al. 2010). Moropoulou et al. (2013) have monitored the preservation state of structural systems and mosaics. Nuzzo et al. (2010) presented the use of GPR in the field of historic building diagnostics, applying it to different constructive elements typical of historic structures. The results have demonstrated the capability of this method to identify essential information for restoration intervention, such as the presence of cracks, fractures and construction techniques. Catapano et al. (2018) have monitored the state of decay of an ancient building, locating several crack patterns affecting the masonry structures, by using a microwave tomographic data processing approach based on GPR surveys. Kanli et al. (2015) have used GPR to monitor restoration works undertaken on an historic building affected by cement injections. They highlighted the importance of using the GPR method to locate fracture zones where restoration was necessary.

### 1.3 ERT and GPR for Monitoring Settlement Phenomena

Settlement represents one of the most dangerous causes of degradation for the stability and safety of civil engineering structures (Handy 2001, 2007). There are many causes that can generate this type of problem, such as weak load-bearing soils, poor compaction of the construction ground, variations in the subsoil water content, the presence of roots, maturing trees and vegetation, non-homogeneous soil consolidation and so on (Budi 2017; Kaliakin 2017; Oh and Vanapalli 2018). In addition, the presence of plumbing leaks and uncompacted hardcore can generate dangerous stability problems and can seriously affect the mechanical behaviour of the building's structure. When settlement occurs, cracks and

fractures can appear on the structures. Reading the distribution of the cracks, in particular where they are concentrated and how they are angled, is an important aid to understanding which kind of movement is occurring. In particular, it is possible to distinguish between vertical translation, horizontal translation, shear deformation, rotation and the combined effects of rotation and translation (Binda and Saisi 2009). It should be noted that even if visible signs of deterioration are detectable on structures, it is very difficult to understand the effects they have on the foundations.

Actually, many systems exist to monitor cracks and fractures occurring in civil engineering structures and infrastructures. The most commonly used are the plastic telltales, consisting of two overlapping plates, one marked with a scale in millimetres fixed on one side of the crack while the other plate is fixed on the opposite side. When settlement occurs, the two plates move in opposite directions making it possible to quantify the displacement by simply reading the millimetre scale. A similar system is composed of a glass telltale fixed with resin to the structure being monitored. At present, the most widely used and advanced system of control is that which uses displacement transducers (Díaz et al. 2018; Sirombo et al. 2017).

However, these methods only allow the study of surface phenomena; no information is obtainable about the soil or the foundations where the settlement occurs. To monitor the behaviour of the building's foundations and to accurately identify the cause of the settlement, it is necessary to discover more about the interaction between the soil and the structure; it is important to note a large number of different types of foundation, depending on the load-bearing capacity of the soil and the type of construction (Chen 1999). The type of soil also varies, as established in the general classification used by geotechnical engineers (ASTM D 2487-00 or D 2488-00). Direct measurements, such as trenches or geotechnical drillings, represent the best approach for investigating the conservation status of foundations subject to decay phenomena, but these are very expensive and invasive. In addition, despite obtaining the information is often time-consuming, it is not able to reveal local variations occurring in the soil.

ERT could be used to support direct measurement for monitoring settlement phenomena. Santarato et al. (2011) used ERT to control the injection of expanding resins during restoration work on buildings where settlement occurred. Furthermore, ERT is particularly useful when analysing the presence of sinkholes and voids that can cause serious risks for the buildings or civil engineering infrastructures (Kaufmann 2014; Perrone et al. 2004, Giampaolo et al. 2016; Naudet et al. 2008; Zini et al. 2015; Samyn et al. 2014). Gómez-Ortiz and Martín-Crespo (2012) have used ERT and GPR to assess the risk of subsidence in a karst environment close to a road. Carbonel et al. (2015) have demonstrated the usefulness of ERT, jointly used with GPR and SAR, to monitor a buried sinkhole cluster in the urban area of Zaragoza (Spain) and confirmed their findings with the use of trenches. The success of ERT for subsurface void detection is highlighted in particular in the study of karstic areas (Zhu and Currens 2011; Guérin et al. 2009, Chamon and Dobereiner 1988).

As regards GPR, because it is able to investigate the subsoil at different depths and in greater detail compared with other non-destructive tests, it is particularly suitable for monitoring the interaction between the ground and the foundations of buildings. Pérez-Gracia et al. (2008) used GPR to identify wet ground areas under the basement of a large block of flats; it enabled the detection of a lack of consistency in thickness of the reinforced concrete slab, and an ancient well that is the probable cause of the damage and the high water content of, the slab. Leucci (2006) used GPR with ERT to investigate a church which suffered from weakened subsoil. The integrated use of geophysical techniques has allowed the detection of the presence of voids that caused the sinking of the floor. Excavations subsequently performed have validated the geophysical measurements. Piscitelli et al.

(2007) identified the cause of subsidence phenomena occurring in an ancient square using GPR microwave tomography and ERT to reconstruct the geometry of a complex system of shallow cavities, partially filled with unconsolidated material, in an urban context. Pueyo-Anchuela et al. (2011) used GPR with seismic measurements and magnetometric acquisitions to survey the subsoil in complex near-surface environments.

Furthermore, in the context of settlement phenomena monitoring, thanks to the possibility of using ERT in boreholes, the method could offer the option of investigating foundations in greater detail than other geophysical techniques, especially when combining the resistivity measurements with electromagnetic and seismic acquisitions. Interestingly, this is the approach described by Wada et al. (2014) who attempted to use a borehole GPR system for detecting voids and studying foundation piles. Kim et al. (2004) used radar borehole measurements integrated with surface ERT to investigate the presence of voids before the construction of a limestone highway bridge. The results obtained are promising and are undoubtedly of interest to those monitoring settlement phenomena.

## 2 Experimental Tests

In order to highlight the importance of the integrated use of ERT and GPR for monitoring the decay occurring in modern building structures, two case studies will be presented and discussed. The results obtained, supported by geotechnical drilling information, have demonstrated the usefulness of an integrated strategy based on geophysical non-invasive tests for studying problems of interest to the field of engineering.

### 2.1 Aims and Objectives

The main objective of the acquisitions was to understand the cause of the observable cracks and survey the subsoil to identify the presence of voids or other type of anomalies in the ground, as well as some water pipe leakage (as stated in Sect. 5), that occurred in the past, with the aim of assessing the vulnerability of the existing structure.

With this aim, we present the results obtained through the joint use of GPR and ERT for the identification of the possible causes of settlement in two civil engineering constructions realized with precast concrete technology and affected by severe examples of degradation to structural and non-structural elements. The data obtained with the two techniques were used for both a simple comparison of the information and to combine the data to increase the quality of the interpretation. Finally, the geophysical results were validated with information obtained by geotechnical drillings.

### 2.2 Case Studies

The first building studied is a warehouse located in the city of Taranto (Puglia Region, Italy) constructed from precast elements and reinforced concrete pile foundations. The site is close to the Mar Piccolo basin, an internal sea located along the Ionian coast in southern Italy (Zuffianò et al. 2016). All piles reach a depth of between 20 and 30 m. The façade elements are made up of concrete panels supported by shallow foundations (depth < 2 m). The foundation soil is comprised of clay and sand.

Some rotational movements have affected the structure, generating cracks and fractures concentrated at the bottom of the façade panels. This type of deterioration has raised

concern among engineers about the safety of the constructions, even though there are no obvious signs of problems with the structural elements.

The second building is adjacent to a bus garage located in the village of Lagonegro (Basilicata Region, Italy) where a great number of cracks and fractures have appeared in the non-structural elements. Since the foundation soil is composed of clay and sandy soils, piles that reach a depth greater than 20 m have also been used. Some non-structural elements (floors and façade panels) contain cracks that have generated justifiable concern about the condition of a building that accommodates both buses and employees.

## 2.3 Data Acquisition

### 2.3.1 Case Study (CS1)

Geophysical investigations were carried out with a multichannel ABEM SAS-1000 georesistivimeter that takes readings using a maximum of 64 electrodes distributed along four cables and is powered by a 12 V battery. A series of holes were drilled into the asphalt layer to insert the electrodes. This step was essential to overcome the electrical insulation caused by the asphalt that would prevent the application of current into the ground. In order to further limit the contact resistance between the electrodes and ground and enhance the quality of the measured data, the holes were also filled with an electrically conductive solution composed of clay (bentonite) and water. GPR measurements were taken to identify the position of any unknown cables or underground utilities in order to avoid damage to these systems.

GPR radargrams close to the façade panels were acquired with a SIR3000 (GSSI Instrument) coupled to a survey wheel and 400 MHz antenna, as indicated by the red line in Fig. 3. One radargram was collected in conjunction with the ERT profile (red line in Fig. 3d) to investigate the decay of the structural elements (i.e. columns and shallow and deep foundations). The frequency of the antenna was selected to provide an acceptable compromise between the resolution and depth of acquisition (Capozzoli and Rizzo 2017). All GPR profiles were acquired by collecting 100 traces per meter. The transmission rate was set to 100 kHz and resolution was equal to 16 bit. No frequency filter or gain functions were adopted during the acquisition phase. The time window was set to 80 ns, and 1024 samples were recorded for tracing.

ERT was performed with the use of 135 electrodes placed as indicated by the blue polygonal line in Fig. 3. The electrodes, spaced 1 m apart, were distributed along two L-shaped lines close to the perimeter of the building where most deterioration had occurred. The theoretical depth of investigation was estimated to be approximately equal to between 5 and 6 m, with an expected vertical resolution of 0.50 m. The data were subsequently inverted with the ERTLab 64 software that allows the easy management of resistivity data acquired in 3D mode (Santarato et al. 2011).

### 2.3.2 Case Study (CS2)

With regard to CS2, two perpendicular lines were investigated with ERT and GPR (see Fig. 4). The ERTs were achieved with only 2D acquisitions, realized according to the Wenner–Schlumberger array with its higher signal strength. This choice was justified because the surveys were carried out in an industrialized area with high background noise. In detail, the first profile (line 1, L1) was used to investigate the slope of the site (direction N–S)
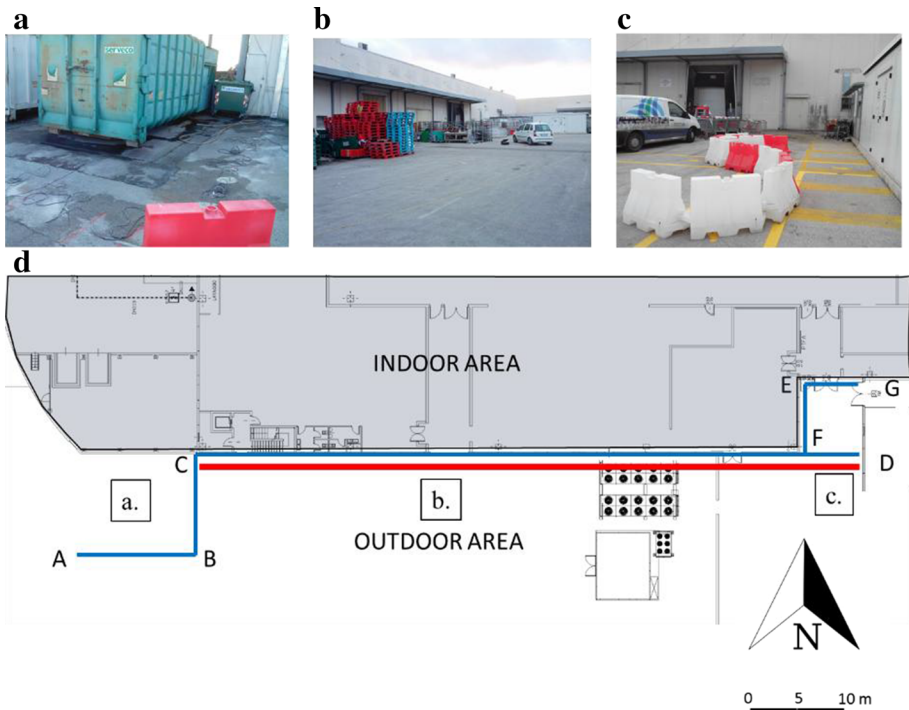
**Fig. 3** Case study (CS1): **a–c** images of the investigated area outside the building; **d** the scheme adopted for ERT (in blue) and GPR (in red) acquisitions with an indication of the location relative to the pictures (**a–c**). As indicated in **d**, the GPR line investigated is located between C and D, while the ERT readings are acquired within the polygon A, B, C, D, E, F, G

while the second profile (line 2) investigated the plane of the site (direction E–W). Since the electrode distance was around 3 m, the depth of investigation was greater than that obtained in CS1. The selected inter-electrode distance enabled the investigation of the presence of anomalies in the soil depth 20–25 m, the depth reached by the foundation piles of the structure.

In addition to these lines, some GPR radargrams were acquired. GPR data were also collected inside the building (see Fig. 4d) to verify the presence of voids caused by settlement occurring in the structure. The instrumentation adopted was the same used for CS1.

## 2.4 Data Processing

### 2.4.1 GPR Data Processing

GPR data were analysed with Reflex-w software (Sandmeier 2013). The processing of the data was based on the use of traditional operations adopted to enhance the depth of investigation and reduce the background noise. In particular, a traditional protocol based on the following steps was followed:
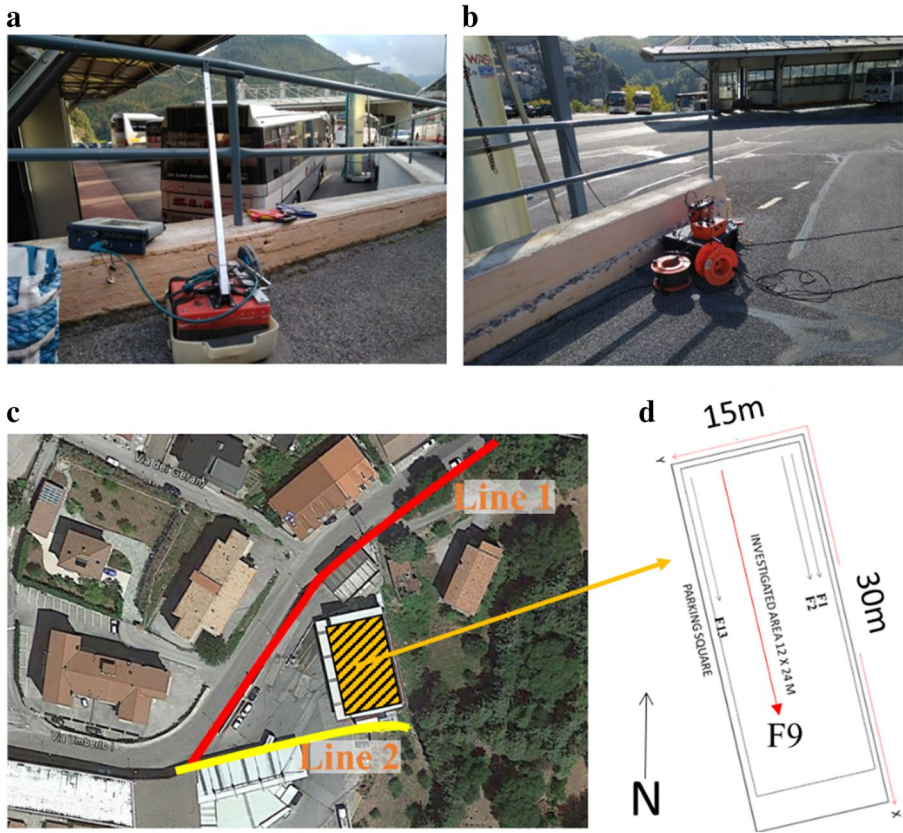
**Fig. 4** CS2: **a** GPR GSSI SIR3000 coupled to a survey wheel and 400 MHz antenna; **b** the georesistivimeter ABEM SAS 1000 coupled to the energy source (12 V lead battery), **c** sketch of the two lines investigated with GPR and ERT: line 1 on the slope and line 2 on the square. The black–yellow rectangle represents the building investigated only with GPR acquisitions made inside the structure; **d** some radargrams are acquired inside the structure, and the positions of the line F9 (the results of which are reported in Fig. 9) are highlighted with the red arrow

1. editing of the data: the coordinates of each radargram were assigned line;
2. moving the start time to remove the unknown signal due to the generation of the EM waves between the interfaces antenna–air;
3. application of a passband filter to retain only the signal ranging between 150 and 1200 MHz to remove low frequency noise and interference;
4. background removal to reduce the ringing noise;
5. application of gain function to increase the investigated depth and quality of detection of anomalies distributed within the soil;
6. a band-pass filter was applied to reduce the noise that increased after the gain function (5);
7. migration of the data with the use of the Kirchhoff algorithm to collapse the reflections induced by spot anomalies in the ground. This operation was made after studying the hyperbolas' reflections, induced by reflectors placed in the ground. This was possible due to the fact that the hyperbolas' shape is regulated by the velocity of the waves in the

soil and geometry of the buried objects. The inclination of the asymptotes is influenced exclusively by the relative permittivity of the medium. The time it takes for the waves to travel to its vertex is a function of the depth of the object, as well as the velocity of the waves entering the ground (Fruhwirth et al. 1996)

### 2.4.2 ERT Data Processing

Two different softwares are used to invert apparent resistivity values recorded in the two test sites, because in the first case (CS1) a 3D acquisition was made, while for CS2, only 2D lines are analysed. In particular, as regards CS1, because of the irregular shape of the building, a 3D ERT was performed in proximity to the foundation structure. The electrodes were placed at a maximum distance of 1 m from the panel or façade, and they were spaced 1 m apart. Three separate readings were made using 64 electrodes each time. In order to compile a 3D electrical resistivity model, all the acquired data were merged with an overlap mode to obtain full disposal data with 135 electrodes. The data were processed with ERTLab (Geostudi Astier srl and Multi-Phase Technologies LLC) that creates a 3D image of the subsoil. After the first elaboration step (filtering and outlier removing analysis), the resistivity inversion software offered a complete three-dimensional model and inversion. The numerical core for the software uses the finite elements (FEM) approach to model the subsoil by adopting a mesh of hexahedrons to correctly incorporate complex terrain topography. The inversion procedure is based on a smoothness-constrained, least-squared algorithm (LaBrecque et al. 1999) with Tikhonov model regularization, where the condition of the minimum roughness of the model is used as a stabilizing function. Throughout the inversion process, the effect of non-Gaussian noise is appropriately managed using a robust data-weighted algorithm (Morelli and LaBrecque 1996).

The total data set (2550 measurements) was inverted by using a mesh with tetrahedral cells ($0.5 \times 0.5 \times 0.25$ m$^3$), a mixed boundary condition (Dirichlet and Neumann) and a starting homogeneous apparent resistivity of 15 Ω m. Both a core and a boundary mesh were generated to accommodate boundary conditions. A 7% standard deviation estimate for noise was assumed to create a data set with a robust inversion. After the inversion routine, a 3D electrical resistivity image was obtained with a low root-mean-square value ($< 5\%$) (Claerbout and Muir 1973; Dahlin and Bernstone 1997).

For CS2, data were processed with ZondRes2D (Zond geophysical software), a computer program for the 2D interpretation of electrical resistivity tomography; a finite-element method is used as the mathematical apparatus to solve forward and inverse. After the analysis and elaboration steps, it was possible to define the real electrical resistivity distribution by the inversion phase of all the apparent resistivity values. The inversion and optimization processes of the recorded values were executed in order to transform the apparent resistivity pseudo-section into a model that represents the distribution of calculated electrical resistivity in the subsurface; The Marquardt classic inversion algorithm consisting of a least-square method using a damping parameter was used. In case of an insufficient quantity of section parameters, this algorithm allows the creation of a contrast subsurface model (Marquardt 1963).

# 3  Results

## 3.1  Case Study

The 3D-ERT is characterized by the presence of some resistive anomalies, with typical dimensions of less than 20 Ω m, placed in a highly conductive background (see Fig. 5a, b). The resistivity values range between 1 and 100 Ω m, the higher values being recorded at the beginning and the end of the investigated polygonal line. Indeed, highly resistive bodies are mostly found in the first 20 m and the last 10 m of acquisition. The electrical anomalies are distributed in the first 2 m of the subsoil, where the highly conductive background is located. Below this first layer, there is a relatively high electrically conductive zone that suggests the presence of a high concentration of water in the subsoil.

The resistive anomalies are also confirmed by the GPR data acquired along the same lines, as shown in Fig. 6. The radargram shows some reflective areas up to a depth of 2 m; in particular, a strong horizontal reflective plane is identified in the first 33 m of the B-scan (anomaly A3) that could be associated with the presence of a different level of soil compaction. Other reflections are detectable at a distance of 43 m (A2) and 60 m (A1) from the starting point of the radargram. The velocity of propagation of the EM waves was equal to 0.085–0.090 m ns$^{-1}$. The radargram shows some reflections associable with the pile foundations (yellow dashed rectangles) and shallow foundations (blue dashed rectangles) that characterize the whole radargram. It is worth noting that the
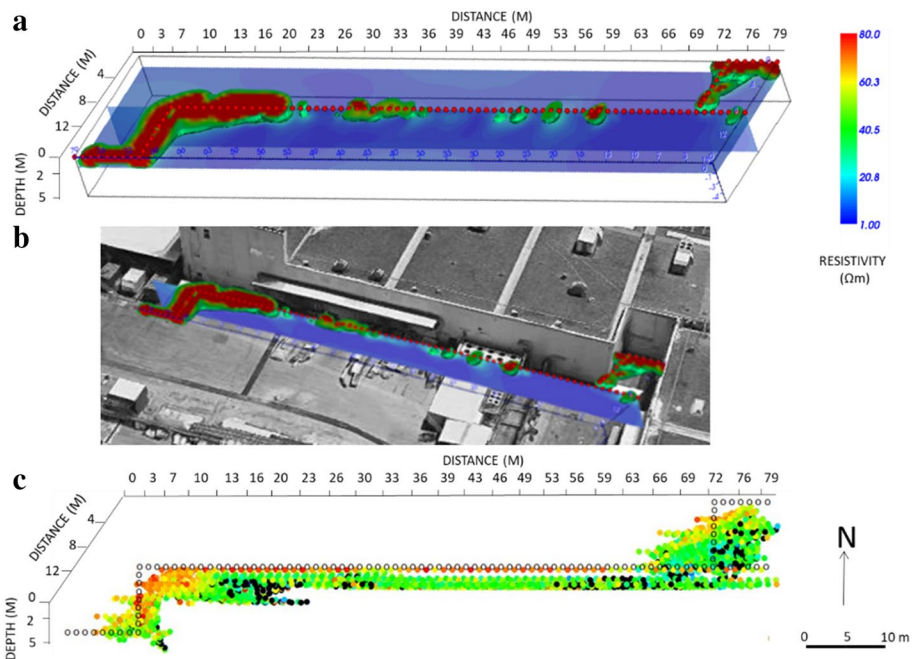


**Fig. 5** 3D ERT results obtained in CS1 (**a**) and in relation to the structure (**b**), the resistivity values are expressed in Ω m, **c** 3D distribution of the recorded resistivity data generated by the 3D L-shape acquisition configuration
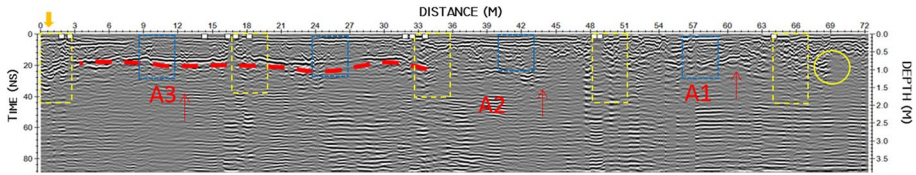
**Fig. 6** Radargram acquired in sector A on the same line investigated with ERT; the position of deep and shallow piles is highlighted with yellow and blue dashed rectangles

anomalies are placed in the immediate vicinity of the shallow foundations, which could be a significant factor in the decay of the structure. Below the first 2 m, a strong attenuation of the signal was recorded.

## 3.2 Case Study

Two ERTs were acquired in the second test site as shown in Fig. 4. The electrical images indicate a geological heterogeneity of the subsoil close to the investigated structure.

The ERT acquired along L1 reached a depth of approximately 20 m. The results showed considerable variation in the data, with the electrical resistivity values ranging between 10 and 500 Ω m. A significant anomaly was recorded by the ERT where decay has occurred under the NW edge of the structure (black dashed lines in Fig. 7a). The electrical anomaly
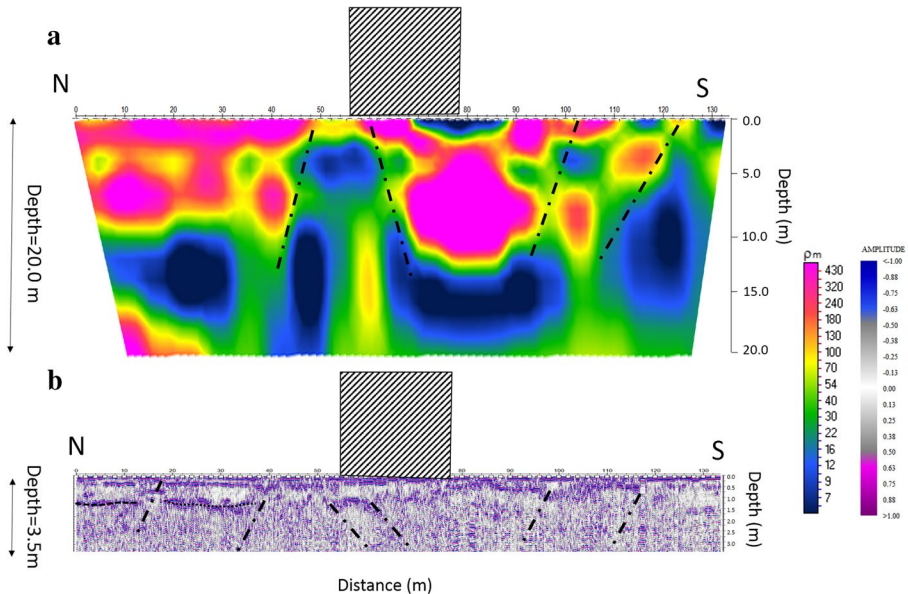


**Fig. 7** Geophysical results obtained in CS2 along L1: **a** ERT results, **b** GPR radargram. The legend plots the resistivity values (ρm) measured by ERT. As can be seen, to simplify the representation and interpretation of the results, the ERT and radargram did not include topographical information. Because the slope is gentle, this simplification is possible since it does not affect the validity of the data. The projection of the area investigated with GPR is plotted with the white dashed rectangle in **a**

was detected at a depth greater than 1 m and is characterized by the presence of conductive and resistive bodies. In addition, the anomaly exists only in the first 10–12 m of the acquisition, indicated by a heterogeneous distribution in the shallower layers of the subsoil. These findings represent the most remarkable results of the ERT and could explain the cause of the decay in the structure. GPR results have shown a large number of reflections that indicate the presence of different layers in the soil (Fig. 7b). The presence of an area characterized by strong attenuation of the EM signal, due perhaps to greater water content, was also detected at a distance of 50–60 m in the same area where ERT revealed the strong electrical anomaly (black dashed lines in Fig. 7b). The depth of investigation of the area was about 3.0–3.5 m, and the EM velocity was evaluated as being 0.09–0.095 m ns$^{-1}$.

The ERT acquired along L2 was performed to survey the area of the square used for bus parking. Here, the site is flat except for the last 20 m, characterized by the presence of an escarpment (that with GPR, for obvious operational problems, was not studied). As plotted in Fig. 8a, the ERT also revealed in this case inconsistent electrical behaviour of the subsoil, particularly in the vicinity of the building, where a strong increase in conductive values was recorded. The first electro-layer is characterized by resistivity values greater than 100 Ω m. Beneath this resistive zone, a less conductive area is recorded where the resistivity values range between 10 and 100 Ω m. The GPR radargram (Fig. 8b) confirmed the presence of the complex physical nature of the subsoil, particularly near the acquisition occupied by the eastern edge of the structure. Indeed, in the last 20 m of the radargram, the recording of a strong attenuation of the GPR signal corresponds to the increase of the conductive behaviour shown by the ERT in the same zone.

GPR information collected inside the structure has excluded the possibility that there are voids under the building, as shown in Fig. 9. The radargram F9 (positioned as indicated in Fig. 4d) identified some reflections due to the presence of connecting beams in the foundations (red rectangles in Fig. 9) and a widespread and significant deformation of
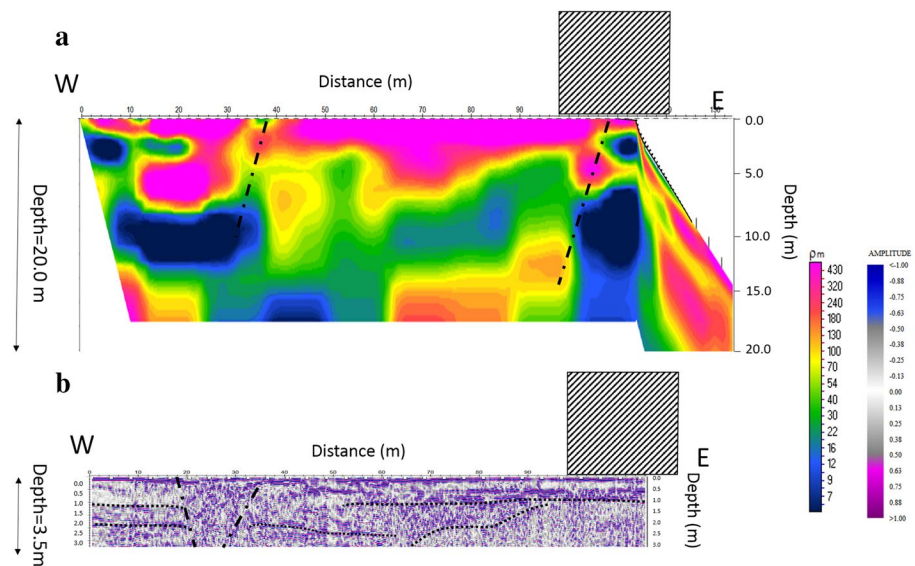


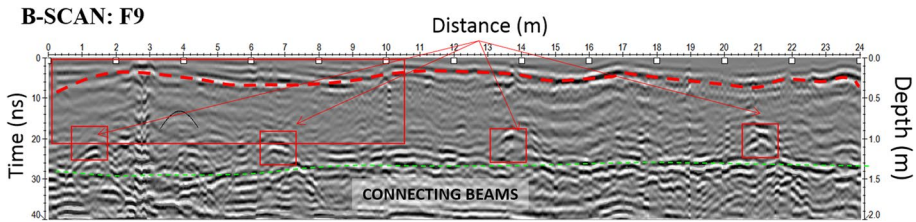**Fig. 8** Geophysical results obtained in CS2 corresponding with L2 with **a** ERT results, **b** GPR radargram

**Fig. 9** B-Scan F9 collected inside the garage (**b**) with its position (**a**). It is possible to see in the radargram (**c**) the presence of the reflectors indicating the presence of the foundations (red rectangles) and two sub-parallel plane reflectors placed at depths of 0.35 m and 1.10 m

the reinforcement [i.e. electrically welded mesh in the concrete slab under the floor that has almost certainly separated from the structural elements (red dashed line)]. No voids or other examples of dangerous decay were detected inside the building as a result of the interpretation of the entire collected data set.

## 4 Discussion

3D-ERT acquired in CS1 has allowed the identification of some resistive nuclei in a conductive background due to the presence of water-saturated soil and clay, as shown in Fig. 3. The results also show the presence of heterogeneous conditions represented by the presence of resistive bodies that could be associated with poor compaction of the subsoil or the use of gravel to level the site before construction of the building commenced. 3D ERT has provided useful information regarding the position of these zones, and the dipole–dipole array used has shown its suitability for acquiring data to help understand the causes of deterioration occurring in the structure. The polygonal line used for the investigation, adopted to overcome the presence of the structure, did not affect the validity of the data. Indeed, the resolution and the depth of investigation match the objective of the measurements. Obviously, the outcome of the investigation was limited, as only information adjacent to the façade could be collected because of the impossibility of inserting electrodes inside the structure.

At the same time, GPR data have identified some significant reflections that could offer a valuable key to identifying the displacement detected between the columns and façade panels of the building. The results, shown in Fig. 3, can be interpreted as presence of poorly-compacted or eroded zones present in the shallow layers of the soil. Indeed, in the vicinity of A1 and A2, GPR has identified some reflections at depths greater than 1 m, immediately below the shallower foundations used to support the façade panels. The obtained results suggest that a settlement phenomenon corresponding with the position of the shallow foundations has occurred, inducing the localized damage observed at the top of the panels. This hypothesis is confirmed by the fact that there is no deterioration in the structural elements (i.e. columns, beams). Below the first 2 m, the presence of reflective layers is worth noting, which is likely due to an increase in clay content within the subsoil.

As shown in Figs. 5 and 6, the foundations (both deep and shallow) have caused high amplitudes and increases in resistivity values, for GPR and ERT data, respectively. The information obtained has demonstrated that the use of the two techniques provides significantly comparable results. A good way to interpret the data is to compare the two images
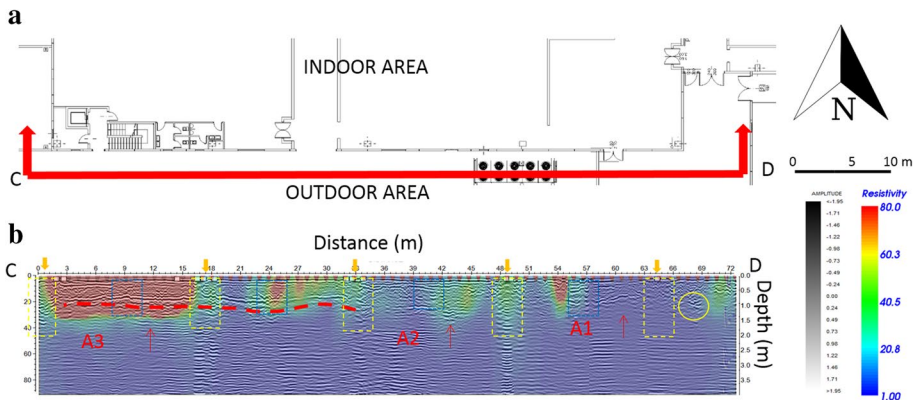
**Fig. 10** Co-rendered image of GPR and a section of the 3D-ERT (**b**) with its location near the building

created for observing the electric and electromagnetic response of the subsoil. Figure 10 comprises a simplified geophysical integration of the two results obtained by a co-rendered image process (Dell'Aversana 2014). The enhanced detail in the image confirms the presence of anomalous events occurring in the subsoil, with an improvement in the final interpretation. The anomalies A2 and A3 are clearly confirmed in both GPR and ERT, while A1 does not correspond to any anomaly in the electrical behaviour of the soil, perhaps due to the resolution of the ERT being significantly less than that obtained with GPR. Figure 10 shows also the electric and electromagnetic contrast that occurred in correspondence of the deep and shallow foundations constituting the structure, highlighted with yellow and blue dashed lines, respectively.

After the geophysical activities, the area was analysed with the aid of four geotechnical drillings that reached a maximum depth of 10 m, three of which were created on the line closest to the most important anomalies investigated with ERT and GPR (see Fig. 11a). On reading the information from the drillings, it was possible to define the geological model of the area (see Fig. 11d), where the presence of layers composed mainly of man-made ground, silty sand and loose gravel was discovered in the first 1–1.50 m. Below the shallower layers, between 1.50 and 3.0 m, saturated sandy loam over silty and sandy loam was detected.

The results obtained, in particular with the core no. 1, showed the unexpected presence in the first meter of uncompacted soil (see Fig. 11b, in conjunction with the first meter drilled—green rectangle). In addition, geotechnical drillings have confirmed the presence of loose material identified by both the ERT results, which identified the presence of resistive anomalies, and the radargram, which detected strong reflections. Finally, the presence of loamy sand and clay matches the conductive behaviour identified by ERT. With the integration of direct and indirect measurements, a new geological model was proposed in order to map the area.

The second test site was studied with an approach based on the use of 2D ERT, collected according to the Wenner–Schlumberger array. The results shown in Figs. 7 and 8 have demonstrated the impressive ability of ERT to portray the subsoil, below the building affected by settlement, at high resolutions. The electrical variations shown in the subsoil are due, in all probability, to the presence of alternating resistive and conductive bodies which are partly the result of work carried out in the past to level the area. The
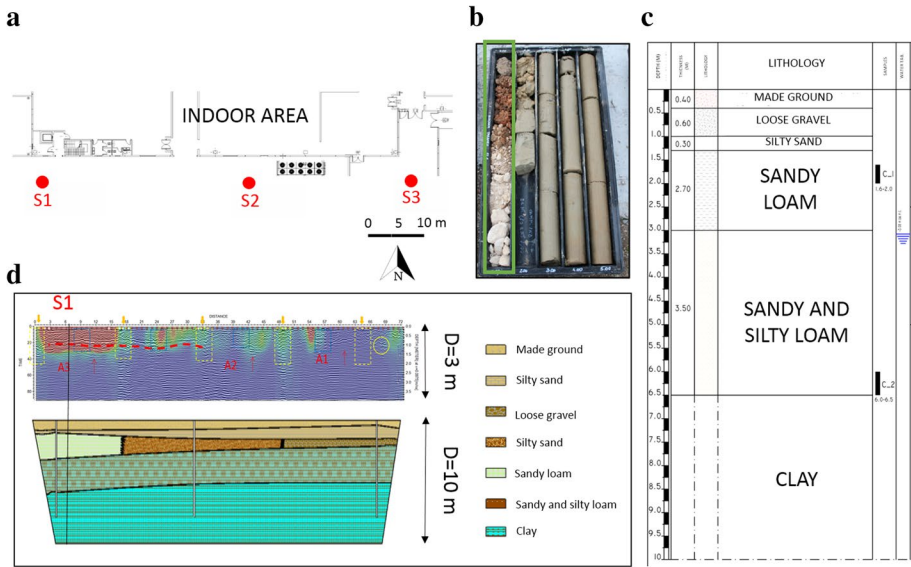
**Fig. 11** Geotechnical drillings carried out in the proximity of the geophysical anomalies: **a** a map of the site with locations of the four drilling points S1–S2–S3–S4 and the line investigated with geophysical methods (red dashed line between the letters X and X′), **b** sampling results obtained in conjunction with the drilling at S1, **c** stratigraphic profile for S1, **d** comparison between the geophysical co-rendered image and resulting geological model
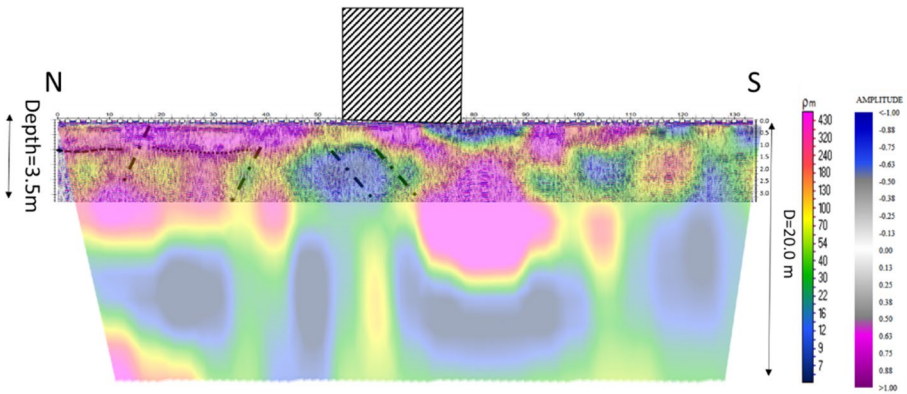


**Fig. 12** Co-rendered image for L1 (CS2) obtained by the overlapping of ERT (false colour) with GPR radargram (blue-purple colours)

good quality of the data has enabled the two images produced with GPR and ERT to be combined, obtaining the integrated data plotted in Figs. 12 and 13. There are an optimal agreement between the two sets of results and a strong correspondence between the electrical and electromagnetic behaviour of the soil. Indeed, where it is possible to identify strong reflections, it is generally possible to detect an increase in resistivity values; the strong attenuation of the GPR signal is related to an increase in electric conductivity
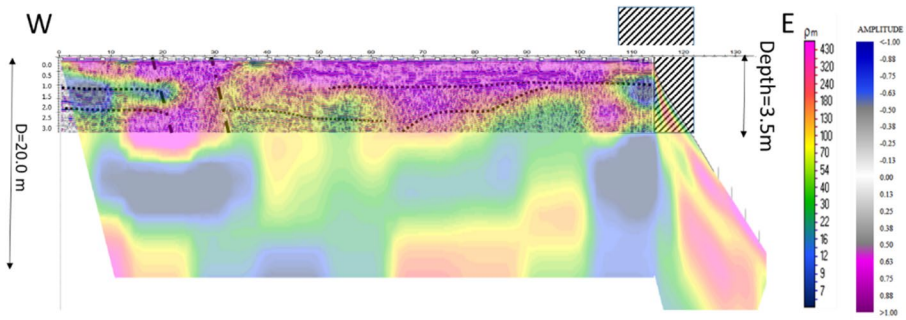
**Fig. 13** L2_ Co-rendered image obtained by the overlapping of ERT (false colour) with GPR radargram (blue-purple colours)

of the soil, as demonstrated at the NW edge of the structure, where the most interesting anomalies are recorded. Other EM reflections are probably related to the geological conditions of the site and engineering works undertaken in the past for levelling the area before the construction of the buildings.

High-amplitude reflections are recorded along L2 (Fig. 8b), and for this reason, it is reasonable to suppose that the soil conditions are drier than those along L1, with the exception of the last 20 m where the radargram shows a strong attenuation of the EM signal. In this last zone, ERT shows the presence of a conductive anomaly that could be associated with higher water content similar to that identified in L1. In this case, the structure is adjacent to the anomaly, particularly the SW edge that does not actually show any sign of deterioration.

ERT revealed the presence of adjacent volumes of conductive and resistive medium due to either varying water content of the soil or alternate layers of rock and sandy soil. Moreover, as for L1, a strong variation in the electromagnetic and electric behaviour was identified adjacent to the edge of the structure where a strong attenuation of the EM signal, and also a conductive volume that returns to the surface, was detected. The results obtained were ideal for co-rendering, to provide a qualitative comparison of the data. As shown in Fig. 13, the overlap of the two geophysical results allows the identification of features in the shallower layer of the subsoil that would be almost undetectable without the integrated use of the two techniques.

The information acquired through geotechnical drillings has, on the one hand, supported the creation of a geological model and, on the other, facilitated the interpretation of the geophysical results. Three geotechnical drillings were undertaken (S1, S2 and S3 in Fig. 14a). From an analysis of the cores, it was possible to identify the presence of different layers: (1) artificially levelled ground that develops for a maximum depth of 3 m; (2) alluvial deposits at depths ranging from the surface down to 20 m; and (3) argillite, marl and calcarenite flysch located at a depth greater than 10 m. The distribution of the three levels is not regular, as demonstrated in the geological model plotted in Fig. 14c, and, obviously, geological conditions have strongly influenced the position of the water table. Indeed, it is possible to note a deepening of the water table close to the S2 bore hole, but this is shallower in the vicinity of S1 and S3 (depth < 6 m). The shapes, portrayed by the geological model, mirror almost exactly the results obtained with geophysical investigations, especially those beneath the building. The compared interpretation of direct and indirect measurements justifies the hypothesis that an
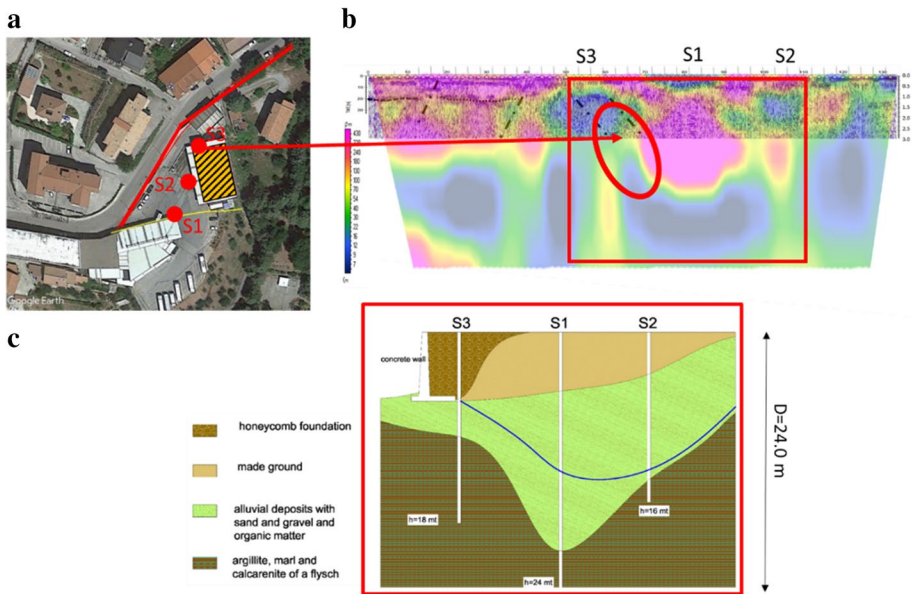
**Fig. 14** Geotechnical drillings operated in CS2 with their locations (**a**), positions compared to the co-rendered geophysical image (**b**) and the resulting geological model obtained using additional geotechnical drilling information (**c**). The geological model relates to the subsoil conditions between the S1 and S3 drillings, while the geophysical results investigated a broader area

irregular distribution of water occurs near the building and that the absence of drainage systems in the area could be the main cause of the induced settlement of the building.

## 5 Conclusions and Future Perspectives

Assessment of the safe conditions of buildings is an essential component of scientific research aiming to provide useful information to support the work of engineers during the design and realization phases of maintenance projects. One of the most important causes of deterioration is the occurrence of settlement, which could be the result of any of a large number of causes. This paper has discussed the applications of ground penetrating radar (GPR) and electrical resistivity tomographies (ERT) for monitoring engineering issues, from the laboratory to the field. As highlighted by the various works discussed, the presence of defects and cracks due to corrosion or mechanical stress causes electrical and electromagnetic variations that can be detected using ERT and GPR. The high resolution of GPR allows the study of microscale effects by analysing the attenuation as well as the velocity propagation of EM signals Resistivity methods can effectively support laboratory tests that monitor electrical effects due mainly to water content variation or the presence of voids. The integration of the two methods is a powerful tool as it reduces the limitations of each, those of depth of investigation (for GPR) and resolution (ERT). Table 2 summarizes a comparison of the applications of ERT and GPR, including an evaluation of the resolution when capturing images of the target, their ability to reach the desired depth and the complexity of their use in the most common applications.

**Table 2** Comparison of ERT and GPR in different areas of interest

| | Engineering | | Geotechnical | | Geological | | Cultural heritage | | Environment | |
| --- | --- | --- | --- | --- | --- | --- | --- | --- | --- | --- |
| | GPR | ERT | GPR | ERT | GPR | ERT | GPR | ERT | GPR | ERT |
| Resolution | +++ | + | ++ | ++ | +++ | +++ | +++ | + | + | ++ |
| Investigation depth | +++ | ++ | + | +++ | + | +++ | ++ | ++ | + | ++ |
| Applicability | ++ | ++ | ++ | ++ | ++ | + | ++ | +++ | ++ | ++ |

+ Low ++ Medium +++ High

For geotechnical and engineering issues, it is clearly necessary to apply both techniques in tandem, in order to minimize the problems inherent to GPR (an inability to reach greater depths) and to ERT (a limit to the obtainable resolution).

With the aim of highlighting the potential of an integrated approach based on the combined use of GPR and ERT, two actual cases of settlement phenomena were monitored.

In the first, results have enabled the possible source of visible cracks to be identified as the lack of consistency of the soil under very shallow foundations affected by a large volume of water in the subsoil. Leakage from pipes and rainwater infiltration could have been the main cause of settlement affecting the structure. Indeed, it is considered that the use of shallow foundations for façade panels has promoted the manifestation of settlement problems, since structural elements supported by deep pile foundations are not affected.

With regard to the second case, the information obtained with the two techniques has allowed the monitoring and categorization of a very complex geological and geotechnical situation that involved the entire structure. The alternating layers of calcarenite, argillite and alluvial deposits, confirmed with the aid of geotechnical drillings, are also highlighted in geophysical investigations that identified the presence of a significant anomaly located just underneath one edge of the structure. The anomaly recorded with both techniques is supposedly associated with insufficient water drainage, made worse by the presence of this same structure that acts as an additional obstacle. In this case, the presence of pile foundations has prevented more serious damage that might have compromised the safety of the building; non-structural components, such as façade panels and floors separated by beams or columns, are affected by cracks due to settlement.

The approach used was based on a comparison of data obtained with each technique, with geotechnical drillings used to collect direct measurements to support the interpretations.

Geophysical results have provided useful proof of the importance of GPR and ERT for understanding the causes of degradation of structures where settlement occurs. The future of these geophysical techniques is based on the quantitative integration of geophysical information, including the use of seismic data, in order to evaluate the safety of old or ancient buildings in non-invasive ways.

# References

Alani AM, Aboutalebi M, Kilic G (2014) Integrated health assessment strategy using NDT for reinforced concrete bridges. NDT&E Int 61:80–94

Annan AP (2005) Ground-penetrating radar. Near surface geophysics, pp 357–438. EISBN: 978-1-56080-171-9 print ISBN: 978-1-56080-130-6 https://doi.org/10.1190/1.9781560801719.ch11

ASTM D2488-00 (2000) Standard practice for description and identification of soils (visual-manual procedure). ASTM International, West Conshohocken. www.astm.org

Benedetto A, Pensa S (2007) Indirect diagnosis of pavement structural damages using surface GPR reflection techniques. J Appl Geophys 62:107–123

Benedetto A, D'Amico F, Fattorini F (2009) Measurement of moisture under road pavement: a new approach based on GPR signal processing in the frequency domain. International Workshop on Advanced Ground Penetrating Radar, Granada

Binda L, Saisi S (2009) Diagnosis and investigation strategy in the assessment of historic buildings. In: Proceedings of 4th international congress on "Science and technology for the Safeguard of Cultural Heritage in the Mediterranean Basin" Cairo Egypt

Binley A, Kemna A (2005) Electrical methods. In: Rubin and Hubbard (eds) Hydrogeophysics. Springer, Berlin, pp 129–156

Bonnet S, Balayssac JB (2018) Combination of the Wenner resistivimeter and Torrent permeameter methods for assessing carbonation depth and saturation level of concrete. Constr Build Mater 188:1149–1165. https://doi.org/10.1016/j.conbuildmat.2018.07.151

Budi GS (2017) Settlement of residential houses supported by piled foundation embedded in expansive soil. Procedia Eng 171:454–460. https://doi.org/10.1016/j.proeng.2017.01.356

Buettner M, Ramirez A, Daily W (1996) Electrical resistance tomography for imaging the spatial distribution of moisture in pavement sections. In: Structural materials technology an NDT conference, San Diego, CA, USA

Capozzoli L, Rizzo E (2017) Combined NDT techniques in civil engineering applications: Laboratory and real test. Constr Build Mater 154:15

Capozzoli L, Caputi A, De Martino G, Giampaolo V, Luongo R, Perciante F, Rizzo E (2015) Electrical and electromagnetic techniques applied to an archaeological framework reconstructed in laboratory. In: Advanced ground penetrating radar (IWAGPR). https://doi.org/10.1109/iwagpr.2015.7292655

Carbonel D, Rodriguez-Tribaldos V, Gutierrez F, Galve JP, Guerrero J, Zarroca M, Roque C, Linares R, McCalpin JP, Acosta E (2015) Investigating a damaging buried sinkhole cluster in an urban area (Zaragoza city, NE Spain) integrating multiple techniques: geomorphological surveys, DInSAR, DEMs, GPR, ERT, and trenching. Geomorphology 229:3–16

Cardarelli E, Di Filippo G, Tuccinardi E (2006) Electrical resistivity tomography to detect buried cavities in Rome: a case study. Near Surf Geophys 4:387–392

Cassidy NJ (2009) Chapter 5—Ground penetrating radar data processing, modelling and analysis. In: Jol HM (ed) Ground penetrating radar theory and applications. Elsevier, Amsterdam, pp 141–176. https://doi.org/10.1016/B978-0-444-53348-7.00005-3

Catapano I, Ludeno G, Soldovieri F, Tosti F, Padeletti G (2018) Structural Assessment via Ground Penetrating Radar at the Consoli Palace of Gubbio (Italy). Remote Sens 10:45

Chamon N, Dobereiner L (1988) An example of the uses of geophysical methods for the investigation of a cavern in sandstones. Bull Int Assoc Eng Geol 38:37–43

Chen FH (1999) Soil engineering, testing, design and remediation. CRC Press, Boca Raton

Claerbout JF, Muir F (1973) Robust modeling with erratic data. Geophysics 38:826–844

Dahlin T, Bernstone C (1997) A roll-along technique for 3D resistivity data acquisition with multi-electrode arrays. In: Proceedings of the SAGEEP'97, vol 2, pp 927–935

Daniels DJ (2004) Ground penetrating radar. In: IEE radar, sonar and navigation series 15. IEE, London

de Groot-Hedlin CD, Constable SC (1990) Occam's inversion to generate smooth, two-dimensional models from magnetotelluric data. Geophysics 55:1613–1624

Dell'Aversana P (2014) Integrated geophysical models. EAGE Book

Dérobert X, Villain G (2017) Effect of water and chloride contents and carbonation on the electromagnetic characterization of concretes on the GPR frequency band through designs of experiment. NDT and E Int 92:187–198

Dérobert X, Aubagnac C, Abraham O (2002) Comparison of NDT techniques on a post-tensioned beam before its autopsy. NDT&E Int 35:541–548

Dérobert X, Iaquinta J, Klyszc G, Balayssac JP (2008) Use of capacitive and GPR techniques for the non-destructive evaluation of cover concrete. NDT&E Int 41:44–52

Dérobert X, Lataste JF, Balayssac JP, Laurens S (2017) Evaluation of chloride contamination in concrete using electromagnetic non-destructive testing methods. NDT&E Int 89:19–29

Díaz E, Robles P, Tomás R (2018) Multitechnical approach for damage assessment and reinforcement of buildings located on subsiding areas: Study case of a 7-story RC building in Murcia (SE Spain). Eng Struct 173:744–757. https://doi.org/10.1016/j.engstruct.2018.07.031

Du Plooy R, Palma Lopes S, Villain G, Dérobert X (2013) Development of a multi-ring resistivity cell and multi-electrode resistivity probe for investigation of cover concrete condition. NDT&E Int 54:27–36. https://doi.org/10.1016/j.ndteint.2012.11.007

Flint RC, Jackson PD, McCann DM (1999) Geophysical imaging inside masonry structures. NDT&E Int 32(8):469–479

Fruhwirth RK, Schmoller R, Oberaigner ER (1996) Some aspects of the estimation of electromagnetic wave velocities. In: Proceedings of the 6th international conference on ground penetrating radar. Tohoku University, Sendai, Japan, pp 135–138

Furman A, Ferré PA, Warrick AW (2003) A sensitivity analysis of electrical resistivity tomography array types using analytical element modeling. Vadose Zone J 2(3):416–423. https://doi.org/10.2113/2.3.416

Giampaolo V, Capozzoli L, Grimaldi S, Rizzo E (2016) Sinkhole risk assessment by ERT: The case study of Sirino Lake (Basilicata, Italy). Geomorphology 253(15):1–9

Gómez-Ortiz D, Martín-Crespo T (2012) Assessing the risk of subsidence of a sinkhole collapse using ground penetrating radar and electrical resistivity tomography. Eng Geol 149–150:1–12

Guérin R, Baltassat JM, Boucher M, Chalikakis K, Galibert PY, Girard JF, Plagnes V, Valois R (2009) Geophysical characterisation of karstic networks—application to the Ouysse system (Poumeyssen, France). CR Geosci 341(10–11):810–817

Handy RL (2001) Does Lateral Stress Really Influence Settlement. J Geotech Geoenviron Eng ASCE 127(7):623–626

Handy RL (2007) Geotechnical engineering: soil and foundation principles and practice, 5th edn. Mcgraw-Hill, New York

Hugenschmidt J, Mastrangelo R (2006) GPR inspection of concrete bridges. Cem Concr Compos 28:384–392. https://doi.org/10.1016/j.cemconcomp.2006.02.016

Hugenschmidt J, Kasa C, Kato H (2013) GPR for the inspection of industrial railway tracks. Near Surf Geophys 11(5):485–491

Hunkeler F (1996) The resistivity of pore water solution—a decisive parameter of rebar corrosion and repair methods. Constr Build Mater 10(5):381–389. https://doi.org/10.1016/0950-0618(95)00029-1

Jol HM (2008) Ground penetrating radar: theory and applications. In: Jol HM (ed) Theory and applications. Elsevier, Amsterdam

Kaliakin VN (2017) Chapter 8—Example problems related to compressibility and settlement of soils. In: Kaliakin VN (ed) Soil mechanics. Butterworth-Heinemann, London, pp 331–376. https://doi.org/10.1016/B978-0-12-804491-9.00008-2

Kanli AI, Taller G, Nagy P, Tildy P, Pronay Z, Toros E (2015) GPR survey for reinforcement of historical heritage construction at fire tower of Sopron. J Appl Geophys 112:79–90

Kaufmann G (2014) Geophysical mapping of solution and collapse sinkholes. J Appl Geophys 111:271–288

Keersmaekers R, Van Rickstal F, Van Gemert D (2004) Geo-electrical techniques as a non-destructive appliance for restoration purposes. In: Modena, Lourenço, Roca (eds) Structural analysis of historical constructions

Keersmaekers DP, Knapen M, Leus M, Van Gemert D (2008) Enhancement of geo-electrical techniques for NDT of masonry. In: D'Ayala D, Fodde E (eds) Structural analysis of historical constructions. Bath, London, pp 1053–1060

Kim JH, Cho SJ, Yi MJ (2004) Borehole radar survey to explore limestone cavities for the construction of a highway bridge. Explor Geophys 35:80–87. https://doi.org/10.1071/EG04080

Krawczyk CM, Polom U, Beilecke T (2013) Shear-wave reflection seismics as a valuable tool for near-surface applications. Lead Edge. https://doi.org/10.1190/tle32030256.1

Lai WWK, Dérobert X, Annan P (2018) A review of ground penetrating radar application in civil engineering: a 30-year journey from locating and testing to imaging and diagnosis. NDT&E Int 96:58–78. https://doi.org/10.1016/j.ndteint.2017.04.002

LaBrecque DJ, Miletto M, Daily W, Ramirez A, Owen E (1996) The effects of noise on Occam's inversion of resistivity tomography data. Geophysics 61(2):538–548

Lapenna V (2016) Resilient and sustainable cities of tomorrow: the role of applied geophysics. Bollettino di Geofisica Teorica ed Applicata 58(4):237–251. https://doi.org/10.4430/bgta0204

Lataste JF, Sirieix C, Breysse D, Frappa M (2003) Electrical resistivity measurement applied to cracking assessment on reinforced concrete structures in civil engineering. NDT&E Int 36(6):383–394. https://doi.org/10.1016/S0963-8695(03)00013-6

Laurens S, El Barrak M, Balayssac JP, Rhazi J (2007) Aptitude of the near-field direct wave of ground-coupled radar antennas for the characterisation of the cover concrete. Constr Build Mater 21(12):2072–2077. https://doi.org/10.1016/j.conbuildmat.2006.05.058

Leucci G (2006) Contribution of ground-penetrating radar and electrical resistivity tomography to identify the cavity and fractures under the main church in Botrugno (Lecce, Italy). J Archaeol Sci 33(9):1194–1204. https://doi.org/10.1016/j.jas.2005.12.009

Liu X, Serhir M, Lambert M (2018) Detectability of junctions of underground electrical cables with a ground penetrating radar: Electromagnetic simulation and experimental measurements. Constr Build Mater 158:1099–1110

Loizos A, Plati A (2007) Accuracy of pavement thicknesses estimation using different ground penetrating radar analysis approaches. NDTE Int 40(2):147–157

Loke MH (2000) Electrical imaging surveys for environmental and engineering studies. A practical guide to 2-D and 3-D surveys

Loperte A, Soldovieri F, Palombo A, Santini F, Lapenna V (2016) An integrated geophysical approach for water infiltration detection and characterization at Monte Cotugno rock-fill dam (southern Italy). Eng Geol 211:162–170. https://doi.org/10.1016/j.enggeo.2016.07.005

Maldague X (2001) Theory and practice of infrared technology for non destructive testing. Wiley, New York, p 684

Marquardt DW (1963) An algorithm for least-squares estimation of nonlinear parameters. J Soc Ind Appl Math 11:431–441

Martel R, Castellazzi P, Gloaguen E, Trépanier L, Garfias J (2018) ERT, GPR, Insar, and tracer tests to characterize karst aquifer systems under urban areas: the case of Quebec City. Geomorphology 310:45–56. https://doi.org/10.1016/j.geomorph.2018.03.003

Martínez K, Mendoza A (2011) Urban seismic site investigations for a new metro in central Copenhagen: near surface imaging using reflection, refraction and VSP methods. Phys Chem Earth A/B/C 36(16):1228–1236. https://doi.org/10.1016/j.pce.2011.01.003

Masini N, Persico R, Rizzo E (2010) Some examples of GPR prospecting for monitoring of the monumental heritage. J Geophys Eng 7:190. https://doi.org/10.1088/1742-2132/7/2/S05

Masini N, Capozzoli L, Romano G, Sieczkowska D, Sileo M, Bastante J, Astete Victoria F, Ziolkowski M, Lasaponara R (2018) Archaeogeophysical based approach for Inca archaeology. Surv Geophys. https://doi.org/10.1007/s10712-018-9502-2

Mokhberi M (2015) Vulnerability evaluation of the urban area using the H/V spectral ratio of microtremors. Int J Disaster Risk Reduct 13:369–374. https://doi.org/10.1016/j.ijdrr.2015.06.012

Moore JC, Pälli A, Ludwing F, Blatter H, Jania J, Gadek B, Glowacki P, Mochnacki D, Isaksson E (1999) High-resolution hydrothermal structure of Hansbreen, Spitsbergen, mapped by ground-penetrating radar. J Glaciol 45:524–532

Morelli G, LaBrecque DJ (1996) Advances in ERT inverse modeling. Eur J Min Geol Eng 1:171–186

Moropoulou A, Labropoulos KC, Delegou ET, Karoglou M, Bakolas A (2013) Nondestructive techniques as a tool for the protection of built cultural heritage. Constr Build Mater 48:1222–1239. https://doi.org/10.1016/j.conbuildmat.2013.03.044

Naudet V, Lazzari M, Perrone A, Loperte A, Piscitelli S, Lapenna V (2008) Integrated geophysical and geomorphological approach to investigate the snowmelt-triggered landslide of Bosco Piccolo village (Basilicata, southern Italy). Eng Geol 98:156–167

Nuzzo L, Calia A, Liberatore D, Masini N, Rizzo E (2010) Integration of ground-penetrating radar, ultrasonic tests and infrared thermography for the analysis of a precious medieval rose window. Adv Geosci 24:69–82. https://doi.org/10.5194/adgeo-24-69-2010

Oh WT, Vanapalli SK (2018) Modelling the stress versus settlement behavior of shallow foundations in unsaturated cohesive soils extending the modified total stress approach. Soils Found 58(2):382–397. https://doi.org/10.1016/j.sandf.2018.02.008

Pérez-Gracia V, García García F, Rodriguez Abad I (2008) GPR evaluation of the damage found in the reinforced concrete base of a block of flats: a case study. NDT & E Int 41(5):341–353. https://doi.org/10.1016/j.ndteint.2008.01.001

Perrone A, Iannuzzi A, Lapenna V, Lorenzo P, Piscitelli S, Rizzo E, Sdao F (2004) High-resolution electrical imaging of the Varco d'Izzo earthflow (southern Italy). J Appl Geophys 56(1):17–29. https://doi.org/10.1016/j.jappgeo.2004.03.004

Piscitelli S, Rizzo E, Cristallo F, Lapenna V, Crocco L, Persico R, Soldovieri F (2007) GPR and microwave tomography for detecting shallow cavities in the historical area of "Sassi of Matera" (southern Italy). Near Surf Geophys 5:275–284. https://doi.org/10.3997/1873-0604.2007009

Plati C, Dérobert X (2015) Inspection procedures for effective GPR sensing and mapping of underground utilities and voids, with a focus to urban areas. In: Benedetto A, Pajewski L (eds) Civil engineering applications of ground penetrating radar. Springer, Berlin

Proto MF et al (2010) Transport infrastructure surveillance and monitoring by electromagnetic sensing: the ISTIMES project. Sensors 10:10620

Pueyo-Anchuela Ó, Casas-Sainz AM, Soriano MA, Pocoví-Juan A (2011) Geophysical techniques applied to urban planning in complex near surface environments. Examples of Zaragoza, NE Spain. Phys Chem Earth A/B/C 36(16):1211–1227. https://doi.org/10.1016/j.pce.2011.05.010

Rizzo E, Santoriello A, Capozzoli L, De Martino G, De Vita CB, Musmeci D, Perciante F (2018) Geophysical survey and archaeological data at Masseria Grasso (Benevento, Italy). Surv Geophys. https://doi.org/10.1007/s10712-018-9494-y

Sagnard F, Norgeot C, Derobert X, Baltazart V, Merliot E, Derkx F, Lebental B (2016) Utility detection and positioning on the urban site sense-city using ground-penetrating radar systems. Measurement 88:318–330. https://doi.org/10.1016/j.measurement.2016.03.044

Samyn K, Mathieu F, Bitri A, Nachbaur A, Closset L (2014) Integrated geophysical approach in assessing karst presence and sinkhole susceptibility along flood-protection dykes of the Loire River, Orléans, France. Eng Geol 183:170–184

Sandmeier KJ (2016) ReflexW version 8.1. Program for processing of seismic, acoustic or electromagnetic reflection, refraction and transmission data. Karlsruhe, Software Manual, pp 628

Santarato G, Ranieri G, Occhi M, Morelli G, Fischanger F, Gualerzi D (2011) Three-dimensional Electrical Resistivity Tomography to control the injection of expanding resins for the treatment and stabilization of foundation soils. Eng Geol 119:18–30. https://doi.org/10.1016/j.enggeo.2011.01.009

Sass O, Viles AH (2006) How wet are these walls? Testing a novel technique for measuring moisture in ruined walls. J Cult Herit 7:257–263

Sass O, Viles AH (2010) Wetting and drying of masonry walls: 2D-resistivity monitoring of driving rain experiments on historic stonework in Oxford, UK. J Appl Geophys 70:72–83

Sevil J, Gutiérrez F, Zarroca M (2017) G Desir, Carbonel D, Guerrero J, Linares R, Roqué C, Fabregat I, Sinkhole investigation in an urban area by trenching in combination with GPR, ERT and high-precision leveling. Mantled evaporite karst of Zaragoza city, NE Spain. Eng Geol 231:9–20

Shangguan P, Al-Qadi IL, Coenen A, Zhao S (2016) Algorithm development for the application of ground-penetrating radar on asphalt pavement compaction monitoring. Int J Pavement Eng 17(3):189–200

Sirombo E, Filippi M, Catalano A, Sica A (2017) Building monitoring system in a large social housing intervention in Northern Italy. Energy Procedia 140:386–397. https://doi.org/10.1016/j.egypro.2017.11.151

Szalai S, Novák A, Szarka L (2011) Which geoelectric array sees the deepest in a noisy environment? Depth of detectability values of multielectrode systems for various two-dimensional models. Phys Chem Earth A/B/C 36(16):1398–1404. https://doi.org/10.1016/j.pce.2011.01.008

Tosti F, Slob EC (2015) Determination, by using GPR, of the volumetric water content in structures, substructures, foundations and soil, civil engineering applications of ground penetrating radar. Springer, Berlin, pp 163–194

Tosti F, Umiliaco A (2014) FDTD Simulation of the GPR signal for preventing the risk of accidents due to pavement damages. Int J Interdiscip Telecommun Netw 6(1):1–9

Tosti F, Bianchini Ciampoli L, D'Amico F, Alani AM (2018) Benedetto, An experimental-based model for the assessment of the mechanical properties of road pavements using ground-penetrating radar. Constr Build Mater 165:966–974

Ungureanu C, Priceputu A, Bugea AL, Chirică A (2017) Use of electric resistivity tomography (ERT) for detecting underground voids on highly anthropized urban construction sites. Procedia Eng 209:202–209. https://doi.org/10.1016/j.proeng.2017.11.148

Van Rickstal F, Van Gemert D, Keersmaekers R, Posen D (2008) Enhancement of geo-electrical techniques for NDT of masonry. In: D'Ayala, Fodde (eds) Structural analysis of historic construction. Taylor & Francis, London

Verma SK, Sharma SP (2011) Urban geophysics. Phys Chem Earth A/B/C 36(16):1209–1210. https://doi.org/10.1016/j.pce.2011.09.007

Viriyametanont K, Laurens S, Klysz G, Balayssac JP, Arliguie G (2008) Radar survey of concrete elements: effect of concrete properties on propagation velocity and time zero. NDT&E Int 41(3):198–207. https://doi.org/10.1016/j.ndteint.2007.10.001

Wada K, Karasawa S, Kawata K, Ebihara S (2014) Small-diameter directional borehole radar system with 3D sensing capability. In: Proceeding of the 15th international conference on ground penetrating radar, GPR. https://doi.org/10.13140/2.1.3105.9207

Williams RA, Stephenson WJ, Odum JK (2006) Seismic imaging in urban areas: examples and lessons learned. In: Symposium on the application of geophysics to environmental and engineering problems, EEGS conference proceedings, 2006 annual meeting, Seattle, Washington, April 2–6, p 10

Wiwattanachang N, Giao PH (2011) Monitoring crack development in fiber concrete beam by using electrical resistivity imaging. J Appl Geophys 75:294–304

Zhu J, Currens JC (2011) Dinger J S, Challenges of using electrical resistivity method to locate karst conduits—a field case in the Inner Bluegrass Region, Kentucky. J Appl Geophys 75:523–530

Zini Z, Calligaris C, Forte E, Petronio E, Zavagno E, Boccali C, Cucchi A (2015) A multidisciplinary approach in sinkhole analysis: the Quinis village case study (NE-Italy). Eng Geol 197:132–144

Zuffianò LE, Basso A, Casarano D, Dragone V, Limoni PP, Romanazzi A, Santaloia F, Polemio M (2016) Coastal hydrogeological system of Mar Piccolo (Taranto, Italy). Environ Sci Pollut Res 23(13):12502–12514